Journal of Translational Medicine

RESEARCH

Open Access

Innovative evaluation of selinexor and JQ1 synergy in leukemia therapy via C-MYC inhibition

Pei-Hong Wang[1*†], Chu-Hong Hu[1†], Jia-Qi Fan[1†], Jia-Jun He[2†], Ting-Fen Deng[1], Yan-Li Xu[1], Yu-Jun Dai[2*] and Shun-Qing Wang[1*]

Abstract

Background Acute myeloid leukemia (AML) remains a therapeutic challenge due to drug resistance and relapse. Selinexor, an XPO1 inhibitor, shows limited efficacy as monotherapy, necessitating combination strategies. JQ1, a BET inhibitor targeting MYC, may synergize with Selinexor to enhance antileukemic effects.

Methods AML cell lines, primary patient samples, and xenograft models (MLL-AF9, CDX, PDX) were treated with Selinexor and JQ1 alone or combined. Synergy was assessed via viability assays (Compusyn/SynergyFinder), apoptosis (flow cytometry/Western blot), and C-MYC suppression (qPCR/CRISPR). In vivo efficacy was evaluated by tumor burden (flow cytometry) and survival.

Results The combination demonstrated strong synergy (CI < 1, HSA > 10) across AML models, with > 80% inhibition in cell lines and primary samples. Mechanistically, it suppressed C-MYC (protein/mRNA), induced apoptosis (cleaved PARP), and arrested cell cycle. In vivo, the combination reduced leukemic burden in bone marrow, spleen, and liver, extending survival in xenografts. PDX models confirmed efficacy in primary AML cells.

Conclusions Selinexor and JQ1 synergistically target AML by dual C-MYC inhibition, offering a promising strategy to overcome resistance. Further clinical evaluation is warranted.

Keywords JQ1, Selinexor, AML, C-MYC, MLL-AF9 bone marrow transplantation model, PDX mouse model

Introduction

Acute myeloid leukemia (AML) is a heterogeneous hematologic malignancy characterized by the clonal expansion of myeloid progenitor cells that fail to differentiate into mature blood cells, leading to the accumulation of immature blasts in the bone marrow and peripheral blood [1]. Despite significant progress in the development of targeted therapies for AML, the prognosis for many patients remains poor, particularly those with adverse genetic mutations or those who relapse after initial treatment [2, 3]. Therefore, there is an urgent need to identify novel therapeutic strategies that can overcome drug resistance and improve patient outcomes.

†Pei-Hong Wang, Chu-Hong Hu, Jia-Qi Fan and Jia-Jun He contributed equally to this work.

*Correspondence:
Pei-Hong Wang
wangph91@163.com
Yu-Jun Dai
daiyj@sysucc.org.cn
Shun-Qing Wang
eywangshq@scut.edu.cn
[1]Department of Hematology, Guangzhou First People's Hospital, Institute of Blood Transfusion and Hematology, Guangzhou Medical University, Guangzhou, Guangdong 500020, China
[2]State Key Laboratory of Oncology in South China, Guangdong Provincial Clinical Research Center for Cancer, Sun Yat-sen University Cancer Center, Guangzhou 510060, P. R. China

Selinexor is a first-in-class selective inhibitor of nuclear export compound that targets the nuclear export protein XPO1 [4]. By inhibiting XPO1, Selinexor prevents the nuclear export of tumor suppressor proteins, transcription factors, and other regulatory molecules, leading to their accumulation in the nucleus and subsequent induction of apoptosis in various cancer cell types, including multiple myeloma, diffuse large B-cell lymphoma, and AML [5–9]. In May 2019, the U.S. Food and Drug Administration (FDA) approved Selinexor in combination with dexamethasone for the treatment of adult patients with relapsed or refractory multiple myeloma who have received at least four prior therapies and whose disease is refractory to at least two proteasome inhibitors, at least two immunomodulatory agents, and an anti-CD38 monoclonal antibody [10].

Although Selinexor has shown single-agent activity in relapsed/refractory AML, with some patients achieving complete remissions, the overall response rates have been modest, and the clinical benefit has been limited to a subset of patients with specific genetic abnormalities, such as TP53 mutations [11]. These findings suggest that while Selinexor has the potential to be an effective therapeutic agent for AML, its efficacy may be enhanced when used in combination with other targeted therapies or conventional chemotherapies [7, 12, 13]. In recent years, there has been growing interest in exploring the potential synergistic effects of combining Selinexor with other agents that target different aspects of AML pathogenesis [14–16]. For example, the combination of Selinexor and FLT3 inhibitors has shown promise in preclinical models of FLT3-mutant AML, suggesting that this combination could be a viable therapeutic strategy for this high-risk patient population [17].

In conclusion, while Selinexor has shown some efficacy in the treatment of AML, its clinical benefit has been limited, highlighting the need for the development of combination therapies that can enhance its activity. Ongoing research efforts are focused on identifying rational combinations of Selinexor with other targeted agents or conventional chemotherapies that can overcome drug resistance and improve patient outcomes in AML.

Materials and methods

Drugs and cell lines

Selinexor、JQ1、Necrostatin-1、Z-VAD-FMK and Ferrostatin-1 were purchased from Targetmol (USA). AML cell lines Kasumi-1 (DSMZ), MOLM13 (DSMZ), MV4-11 (ATCC), THP-1 (ATCC), OCI-AML2 (DSMZ), HL60 (ATCC) and U937 (DSMZ) were cultured according to the manufacture's instruction.

Primary samples

Human bone marrow (BM) samples of AML patients were collected in accordance with the Declaration of Helsinki, and all manipulations were approved by the Institutional Review Board of Guangzhou First People's Hospital, School of Medicine, South China University of Technology. All the patients have signed the informed consents. Mononuclear cells were separated from BM samples by Lymphoprep™ (STEMCELL Technologies, Canada) using density gradient certification. The mononuclear cells were cultured in StemSpan™ SFEM II medium (STEMCELL Technologies, Canada) supplemented with 10 ng/mL rh-SCF, 10 ng/mL human IL3, 10 ng/mL human IL6 (all cytokines were purchased from R&D Systems, USA).

Virus production and transduction of cells

The plasmids of MSCV-MLL/AF9-IRES-eGFP were constructed as previously described [18]. MSCV-MLL/AF9-IRES-eGFP and Ecopack packaging vector were co-transfected into 293T cells to produce retroviruses using Lipofectamine™ 3000 (Thermo Fisher Scientific, USA). The guide RNAs (sgRNA) targeting human BRD4 (sgRNA-*BRD4*-1 5′-CACCGCTGGGTGCTGCTGA GAGTC-3′, sgRNA-*BRD4*-2 5′-CACCGTGCTGCAG CGGCATCCTCA-3′) for CRISPR-Cas9 gene knockout were designed using Benchling online tools (https://benchling.com/crispr). The sgRNA were cloned into the LentiGuide-Puro plasmid (52963, Addgene) according to the previous publication [19]. LentiGuide-Puro plasmid targeting BRD4 and packaging vector pSPAX2 (12260, Addgene), pMD2G (12259, Addgene) were co-transfected into 293T cells to produce sgRNA lentivirus. LentiCas9-Blast (52962, Addgene) and packaging vector pSPAX2, pMD2G were also co-transfected into 293T cells to produce Cas9 lentivirus. Viral supernatant was collected 48 h after transfection. For transduction of bone marrow cells, 800 μl retroviruses were mixed with 200 μl of cell cultured in RPMI1640 media plus 10% FBS, 1% penicillin/streptomycin (Yeasen, china), 10 ng/mL of IL-3 and IL-6, 40 ng/mL SCF, and 20 ng/mL Flt3 ligand (all cytokines were purchased from R&D Systems, USA), then polybrene (Yeasen, China) were added into the mixture at a final concentration of 5 μg/mL. For transductions of cell lines, 4.0×106 cells in 2 mL media were mixed with 2 mL of viral supernatant and polybrene were added into the mixture at a final concentration of 10 μg/mL. The mixture of cells and viruses were certificated at 1200 g for 90 min at 37 °C for transduction. Cas9 lentivirus was firstly used to infect MOLM13, MV4-11 and THP-1cells. 48 h after infection, 10 μg/mL blasticidin S HCl (Beyotime, China) were added to the culture for 3 weeks and the alive cells were infected with sgRNA lentivirus. Then the cells were incubated with 1 μg/

mL puromycin dihydrochloride (Beyotime, China) for a week. The knockout of BRD4 in surviving cells was verified by western blots. MOLM13 cells were transduced with MSCV-C-MYC-IRES-GFP lentivirus to overexpress C-MYC, with empty MIGR1 vector as control. GFP^+ cells were sorted by flow cytometry 72 h post-transduction to enrich transfected populations. Post-sorting, protein lysates were subjected to Western blot (WB) using anti-C-MYC antibody to confirm elevated C-MYC expression.

Cell viability assay

AML cells (3000 cells per well for AML cell lines, 20000 cells per well for primary cells) were seeded into 96-well plates and incubated with Selinexor (1.52 nM to 10000 nM, 1:3 dilution rate), JQ1 (1.52 nM to 1000 nM, 1:3 dilution rate) or the two drugs at the indicated concentration for 48 h. Then cell viabilities were detected following the instruction of CellTiter-Glo® 2.0 Cell Viability Assay (Promega, USA). The relative cell viabilities were normalized to the untreated controls. The 50% inhibitory concentration (IC50 values) for each drug was calculated by nonlinear best-fit regression analysis in GraphPad Prism v.9 software. The combination index (CI) of Selinexor and JQ1 was quantified using Compusyn Software: CI < 1 synergism and CI > 1 antagonism. The Highest Single Agent (HSA) score of the two drugs was quantified using the online tools SynergyFinder (https://synergyfinder.org/) and HSA > 10 means synergism.

Cell cycle and cell apoptosis analyses

For cell apoptosis assays, cells (2×10^5 per well) were treated with drugs at the indicated concentrations for 48 h in 6-well plates. The proportion of apoptotic cells were labeled with APC Annexin V Apoptosis Detection Kit with PI (BioLegend, USA) following the instruction and then detected by flow cytometry (BD LSRFortessa™ X-20, USA). The treated cells were also lysed to collect protein for western blot analysis. For cell cycle analysis, cells (2×10^5 per well) were treated with drugs at the indicated concentrations for 24 h in 6-well plates. The treated cells were stained with Cell Cycle and Apoptosis Analysis Kit (Yeasen, China) as the instruction recommended and then analyzed by flow cytometry (BD LSRFortessa™ X-20, USA).

EdU incorporation analysis

The AML cell lines MOLM113, MV4-11, and Kasumi-1 were seeded in 6-well plates at a density of $0.5–1 \times 10^6$ cells/well and treated for 48 h with control (DMSO vehicle), 50 nM Selinexor, 50 nM JQ1, or their combination. Two hours before harvesting, 1 mM EdU (Beyotime C0071S) was added to the culture to label proliferating cells. Cells were collected by centrifugation, stained with Annexin V-APC to detect apoptosis, and then fixed/permeabilized following the EdU kit protocol (Beyotime C0071S). EdU incorporation was labeled with FITC to quantify cell cycle phases (G1, S, G2/M). Annexin V-APC (apoptosis) and EdU-FITC (S-phase) signals were detected and analyzed by flow cytometry (BD LSRFortessa™ X-20, USA).

RNA extraction and RT-qPCR

The AML cell lines MOLM13 and MV4-11 were seeded in 6-well plates at a density of $0.5–1 \times 10^6$ cells/well and treated for 24 h with control (DMSO vehicle), 50 nM Selinexor, 50 nM JQ1, or their combination. Cells were pelleted by centrifugation, and total RNA was extracted using TRIzol reagent (Invitrogen) followed by chloroform phase separation and isopropanol precipitation. RNA purity and concentration were measured using a NanoDrop spectrophotometer.

Reverse transcription was performed with 1 μg of RNA using the High-Capacity cDNA Reverse Transcription Kit (Takara, RR036A). Quantitative PCR was carried out on an ABI 7500 Real-Time PCR System (Applied Biosystems) using SYBR qPCR Master Mix (Vazyme, Q711). Gene-specific primers for C-MYC (forward: GGCTCCT GGCAAAAGGTCA; reverse: CTGCGTAGTTGTGCTG ATGT) and GAPDH (forward: GAAGGTGAAGGTCGG AGTC; reverse: GAAGATGGTGATGGGATTTC) were used to amplify target sequences. Gene expression data were normalized to GAPDH as an internal control, and relative fold changes were calculated using the 2^(-ΔΔCt) method.

Western blots

After incubating with Selinexor or JQ1 for 24–48 h, the AML cells were washed with PBS and counted by Countess 3 Automated Cell Counter (Thermo Fisher Scientific, USA). Then the cells were lysed with Laemmli 2×concentrated sample buffer (Sigma-Aldrich, Germany) according to the instructions and then immunoblotting was conducted as previously described. The following antibodies were used: PARP1 (#13371-1-AP, Proteintech, USA), caspase8 (#13423-1-AP, Proteintech, USA), c-Myc-ChIP Grade (#ab32072, abcam, UK), HRP-conjugated GAPDH Monoclonal antibody (#HRP-60004, proteintech, USA), Anti-rabbit IgG, HRP-linked Antibody (#7074, CST, USA).

Animal experiments

Six-week-old female C57BL/6J mice (Charles River, China) were euthanized and the BM cells were collected from the tibia and femur. Then the BM cells were infected with retrovirus of MSCV-MLL/AF9-IRES-eGFP for 48 h. In primary transplants, the infected cells were injected into lethally irradiated (9.5 Gy) recipients (2.5×10^6 per mouse) via tail vein. When the mice displayed signs of

distress/disease, they were sacrificed and BM cells were collected. In secondary transplants, the BM cells of primary recipients were transferred into secondary recipients (5×10^5 per mouse). 3 days after injection, the mice were randomly divided into four groups to receive drug treatment or vehicle control for a total of 9 days: vehicle, Selinexor (10 mg/kg, gavage every other day), JQ1 (40 mg/kg, gavage, a 5-day on/2-day off dosing regimen) or Selinex + JQ1. 12 days after cell injection, the percentage of leukemic cells (GFP^+ cells) in the peripheral blood (PB) were detected by flow cytometry (BD LSRFortessa™ X-20, USA). 14 days after cell injection, 3 mice of each group were sacrificed and BM, spleen (SP) and liver cells were collected. The percentage of leukemic cells in BM, SP and liver was detected by flow cytometry (BD LSRFortessa™ X-20, USA). The spleens and livers of one mouse in each group were further analyzed by hematoxylin-eosin (H&E) staining.

Human AML cell line MOLM13 (2×10^6) was intravenously injected into busulfan-preconditioned (5 mg/kg) C-NKG mice(Cyagen, China). After 4 days, mice were randomized into control, selinexor (10 mg/kg, gavage every other day), JQ1 (40 mg/kg, a 5-day on/2-day off oral dosing regimen), or combination groups for 2 weeks. Peripheral blood was collected post-treatment for preliminary analysis. On day 18, bone marrow and spleen cells were harvested, stained with anti-human CD45 antibody (BioLegend), and analyzed by flow cytometry to quantify $hCD45^+$ leukemia cell engraftment. Spleens were selected for H&E staining and hCD45 immunohistochemistry (IHC) using anti-human CD45 antibody.

For patient-derived xenografts (PDX), primary AML cells (2×10^6 per mouse) were injected into six-week-old female NOG mice (Charles River, China) treated with busulfan (30 mg/kg, Merck, Germany) via tail vein. When the mice (P0 NOG) displayed signs of distress/disease, they were sacrificed and BM cells were collected for secondary transplantation. In secondary transplants, the BM cells of P0 NOG (5×10^5 per mouse) were injected into NOG mice (P1 NOG) treated with busulfan (30 mg/kg, Merck, Germany). 3 weeks after injection, the mice were randomly divided into four groups to receive drug treatment or vehicle control for a total of 21 days: vehicle, Selinexor (10 mg/kg, gavage every other day), JQ1 (40 mg/kg, gavage, a 5-day on/2-day off oral dosing regimen) or Selinexor with JQ1. The leukemic cells (human $CD45^+$ cells) in PB were stained with APC anti-human CD45 (clone: HI30, biolegend, USA) and then were analyzed by flow cytomentry (BD LSRFortessa™ X-20, USA) at the end of the treatment. When the mice (P1 NOG) displayed signs of distress/disease, 3 mice in each group were sacrificed and BM and SP cells were collected. The SP was weighted. The percentage of leukemic cells (human $CD45^+$ cells) in BM and SP were analyzed by flow cytomentry. All the animal experiments were approved by the Animal Ethics Committee at South China University of Technology. This study complied with all relevant ethical regulations regarding animal research.

Statistical analyses

Data are presented as mean plus or minus standard error of the mean. P values were analyzed utilizing the paired or unpaired 2-tailed Student's t-test. Statistical significance is expressed as p value ($^*p \le 0.05$; $^{**}p \le 0.01$; $^{***}p \le 0.001$).

Results

Selinexor and JQ1 synergistically kill AML cells

To further enhance the efficacy of Selinexor, we identified through high-throughput drug screening (300 compounds in the L2100 library) that JQ1 can significantly potentiate the effects of Selinexor. Subsequently, we conducted validations across a panel of leukemia cell lines. Initially, we assessed the synergistic efficacy of the Selinexor and JQ1 in Kasumi-1 and MOLM13 cells (Fig. 1A-H). The findings demonstrated that both Selinexor and JQ1, when administered as single agents, could effectively induce cytotoxicity in these two acute myeloid leukemia (AML) cell lines, with their potency increasing in a concentration-dependent manner. Notably, the combinatorial application of these two drugs exhibited significantly enhanced cytotoxic effects compared to their individual usage (Fig. 1A and E). A heatmap illustrated the inhibitory rates of Selinexor and JQ1 at various concentrations against the AML cell lines. Across all cell lines tested, the half-maximal inhibitory concentration (IC50) values for both Selinexor and JQ1 were showed in Figure S1A and S1B. Specifically, in Kasumi-1 cells, the combined inhibitory rate of high dose of Selinexor (at 120 nM) and JQ1 (at 80 nM) exceeded 85%, while in MOLM13, the combined inhibitory rate of Selinexor (at 160 nM) and JQ1 (at 100 nM) reached approximately 80% (Fig. 1B and F). Furthermore, we employed Compusyn Software to precisely calculate the combination index (CI) of Selinexor and JQ1, revealing significant synergistic interactions between these two agents in both cell lines ($CI < 1$) (Fig. 1C and G). Additionally, the Highest Single Agent (HSA) scores for these two drugs were computed using SynergyFinder (https://synergyfinder.org/), yielding values of 15.761 and 14.186 in Kasumi-1 and MOLM-13 cells, respectively (Fig. 1D and H). We further validated our findings in MV4-11, THP1, OCI-AML2, HL60 and U937 cell lines, and similar results were obtained (Fig. 1I and P and Figure S2). Specifically, the Highest Single Agent (HSA) scores for these two drugs in MV4-11 and THP-1 cells were 22.738 and 12.316, respectively (Fig. 1L and P).

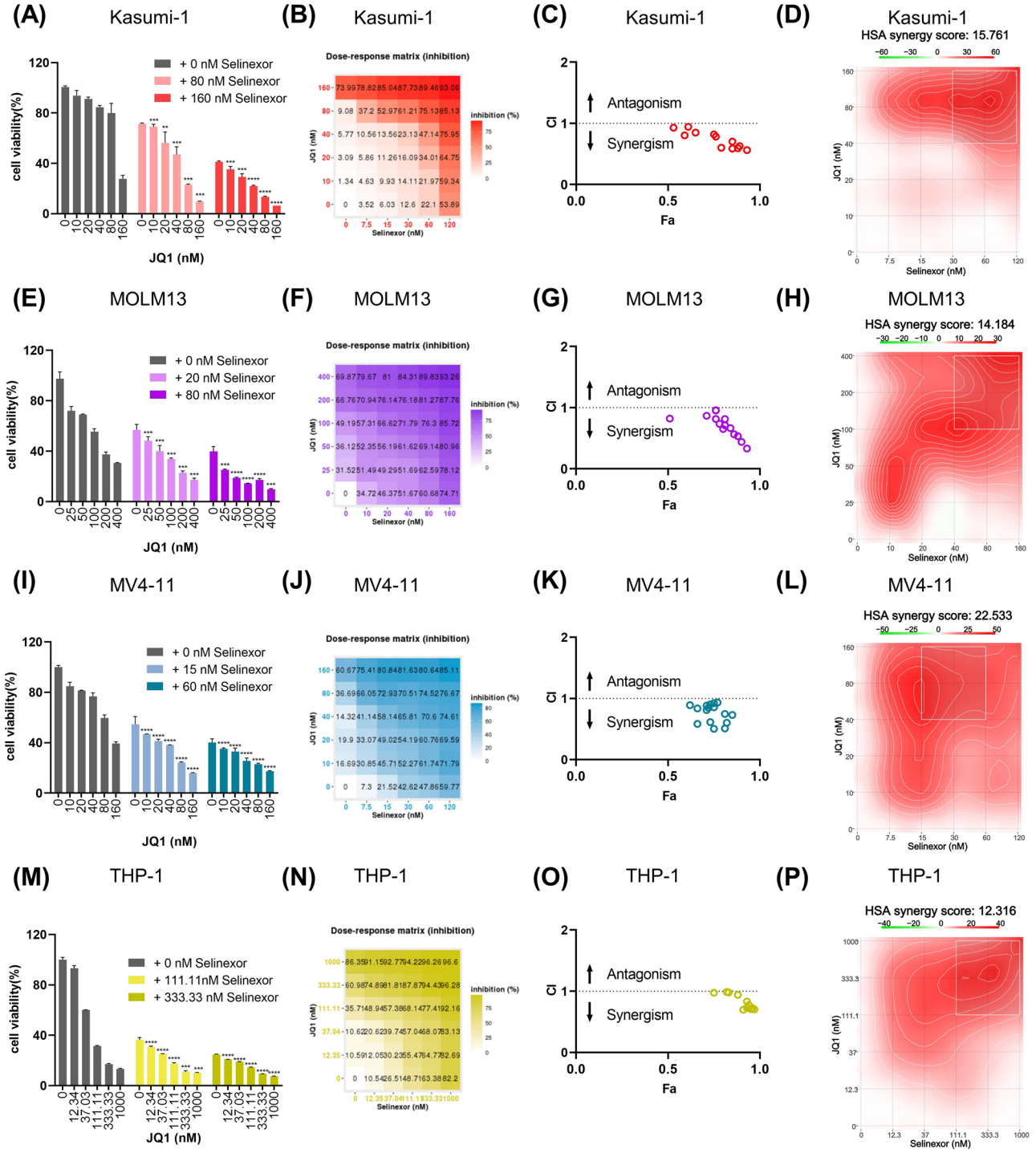

Fig. 1 , Selinexor and JQ1 synergistically kill AML cells. Cell viability assays under the influence of different concentrations of Selinexor and JQ1, respectively in cells Kasumi-1 (**A**), MOLM13 (**E**), MV4-11 (**I**) and THP1 (**M**). Inhibition rate heat map at different concentrations of Selinexor and JQ1, respectively in cells Kasumi-1 (**B**), MOLM13 (**F**), MV4-11 (**J**) and THP1 (**N**). Drug synergy index at different concentrations of Selinexor and JQ1 in different AML cells, respectively in cells Kasumi-1 (**C**), MOLM13 (**G**), MV4-11 (**K**) and THP1 (**O**). The Highest Single Agent (HSA) scores for these two drugs in Kasumi-1 (**D**), MOLM13 (H), MV4-11 (**L**) and THP1 (**P**). All experiments were performed with at least three independent replicates

Subsequently, our investigation focused on the quantification of apoptotic indices and the assessment of cell cycle dynamics in leukemia cells subsequent to pharmacological intervention. As rightly noted, while higher concentrations were discussed initially, we subsequently adopted more physiologically relevant doses: primary working concentration (50 nM). Utilizing Western Blot (WB) analysis, we identified a profound upregulation in the expression levels of PARP and its cleaved fragment, cleaved-PARP, within tumor cells exposed to drug treatment. Notably, the combinatorial application of both drugs resulted in a synergistic enhancement of PARP protein expression (Fig. 2A-C). These findings implicate that the administration of these drugs, especially in combination, elicits a pro-apoptotic response in neoplastic cells. To further substantiate these results, we conducted flow cytometric analysis using PI-ANNEXIN V staining to directly quantify the proportion of cells undergoing apoptosis and necrosis (Fig. 2D and G). These data provided confirmatory evidence, demonstrating a significant escalation in the frequency of apoptosis induction under combinatorial drug therapy compared to monotherapy or untreated controls. To investigate the tumor cell death mechanisms induced by the JQ1-Selinexor combination therapy, we treated the combination therapy group with inhibitors of apoptosis, necrosis, and autophagy, respectively. The results showed that the apoptosis inhibitor significantly suppressed cell death, suggesting that the primary cell death type induced by the combination therapy was apoptosis (Figure S3). Furthermore, the cell cycle results showed that after drug treatment, the proportion of cells in the actively proliferating S phase became increasingly smaller (Fig. 2H). Our 48-hour EdU incorporation assay revealed that only a minority of cells in the combination treatment group retained EdU labeling. The co-staining results demonstrated that apoptotic cells were EdU-negative, indicating that the combination therapy might work through cell cycle arrest. (Figure S4).

JQ1 and Selinexor jointly inhibit the expression of C-MYC

Preliminary research has indicated that JQ1 is capable of inhibiting the expression of MYC, while Selinexor can also suppress MYC at the protein level [7, 20]. Consequently, we hypothesized that JQ1 and Selinexor enhance their anti-tumor effects by concurrently inhibiting the expression mechanism of C-MYC. We treated Kasumi-1, MV4-11, and THP-1 cells with JQ1 and Selinexor for 24 and 48 h, respectively, and subsequently assessed the changes in MYC expression levels. The results from our cellular experiments supported our hypothesis, revealing a further significant reduction in MYC protein expression levels following the combined use of both drugs (Fig. 3A-B and S5). JQ1 is a selective inhibitor of BRD4; therefore, we employed CRISPR technology to knock down BRD4 in MOLM13, MV4-11 and THP-1 cells using two different sgRNAs (Fig. 3C and F and S5). We observed that knocking down BRD4 led to a significant decrease in MYC protein expression (Fig. 3E and H and S5). Moreover, the modified cell lines exhibited a increase in sensitivity to Selinexor, with a reduced IC50 value for Selinexor (Fig. 3C, D, F and G and S5). After overexpressing c-MYC in MOLM13 cells, we treated them with the combination therapy. The results demonstrated a significant reduction in the cytotoxic efficacy of the drug combination against the modified cells, further supporting c-MYC as a key target of the combined treatment (Fig. 3I, J). We further analyzed the c-MYC RNA levels and the results showed a pronounced reduction in c-MYC RNA levels in the combination therapy group compared to monotherapy groups. This suggests that the drug combination may exert its effects through modulation of c-MYC transcript levels, with the underlying mechanisms requiring further investigation (Fig. 3K, L).

Killing of Leukemia Cells by JQ1 and Selinexor in vivo

To further verify the effects of JQ1 and Selinexor in vivo, we constructed an MLL-AF9 bone marrow transplantation model through lentivirus-mediated hematopoietic stem cell bone marrow transplantation, as shown in Fig. 4A. We began administering drugs to the second-generation transplanted mice on the third day, and tested the tumor burden indicators of the mice around two weeks later. The results in mice showed that after administration, the change in overall body weight of the mice was little (Figure S6A). The proportion of GFP-positive tumor cells in the peripheral blood and bone marrow of the mice decreased to varying degrees, among which the combined group of JQ1 and Selinexor had the strongest tumor cell killing effect (Fig. 4B and C and Figure S6C). We further examined the proportion of tumor cells in hematopoietic tissues outside the bone marrow, such as the spleen and liver, and found that JQ1 is highly effective in killing tumor cells outside the bone marrow. The number of GFP-positive tumor cells in the spleen and liver was significantly reduced. Moreover, when combined with selinexor, almost all tumor cells outside the bone marrow could be completely eradicated (Fig. 4D and E and Figure S6C). Pathological sections of the spleen and liver tissues also indicated a significant reduction in tumor cell infiltration after medication, and the tissue structure gradually returned to normal after treatment (Fig. 4F). There were also significant differences in the weight and size of the spleen before and after medication, especially after the combined use of the two drugs, the weight and size of the spleen approached the levels of normal mice (Fig. 4G and H). The mouse survival curve suggested that the use of JQ1 or selinexor could significantly prolong the survival of mice, and the survival time

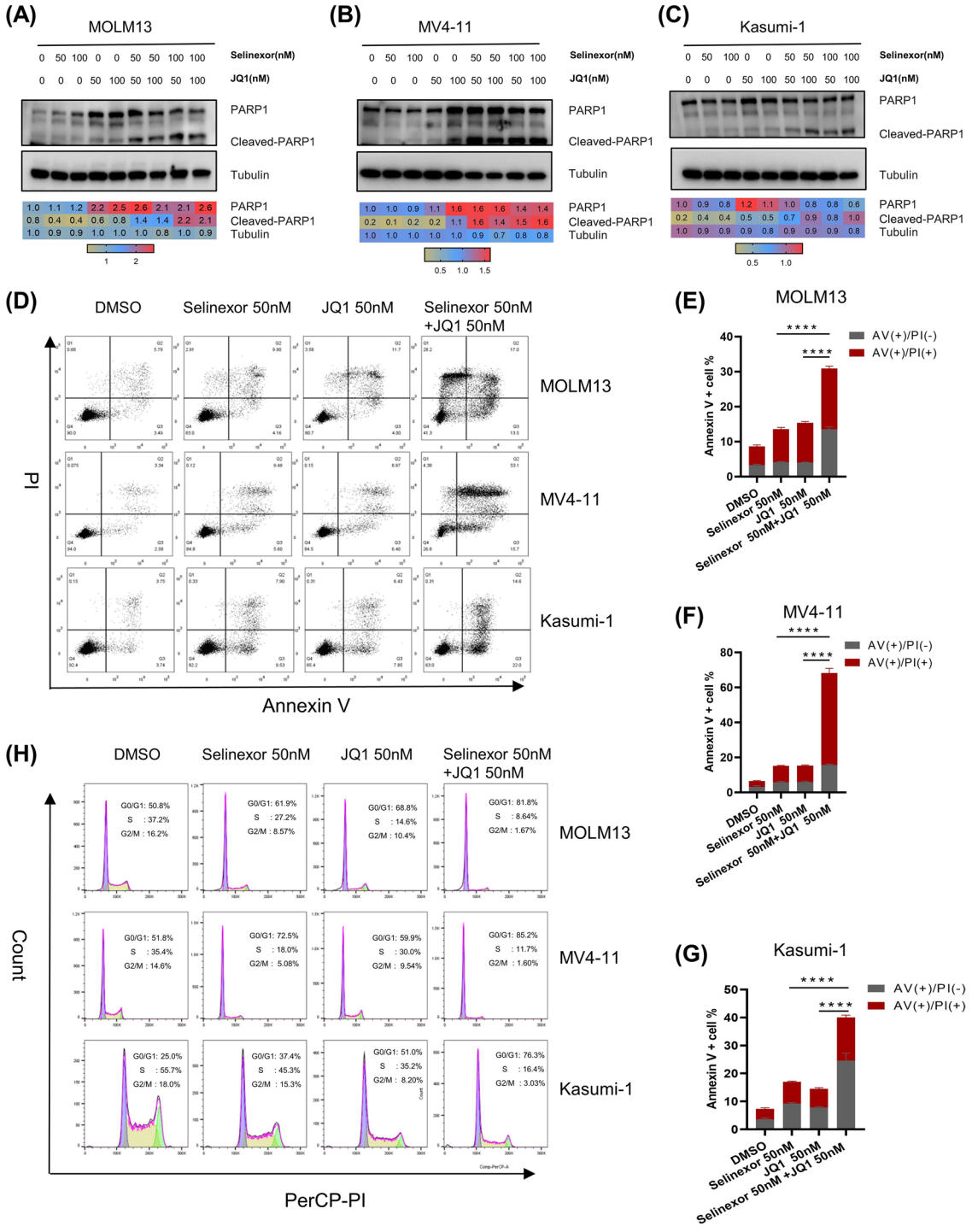

Fig. 2 , Cell cycle and apoptosis of Selinexor and JQ1 in AML cells. (**A**-**C**) Expression levels of apoptotic protein PARP and cleaved PARP at different concentrations of Selinexor and JQ1 in AML cells, respectively in cells MOLM13 (**A**), MV4-11 (**B**) and Kasumi-1 (**C**). (**D**) Apoptosis scatter plots of Selinexor (50nM) and JQ1 (50nM) in AML cells, respectively in cells MOLM13, MV4-11 and Kasumi-1. (**E**-**G**) Apoptosis bar charts of Selinexor (50nM) and JQ1 (50nM) in AML cells, respectively in cells MOLM13 (**E**), MV4-11 (**F**) and Kasumi-1 (**G**). (**H**) Cell cycle detection in AML cells before and after treatment with Selinexor (50nM) and JQ1 (50nM), respectively in cells MOLM13, MV4-11 and Kasumi-1. All experiments were performed with at least three independent replicates

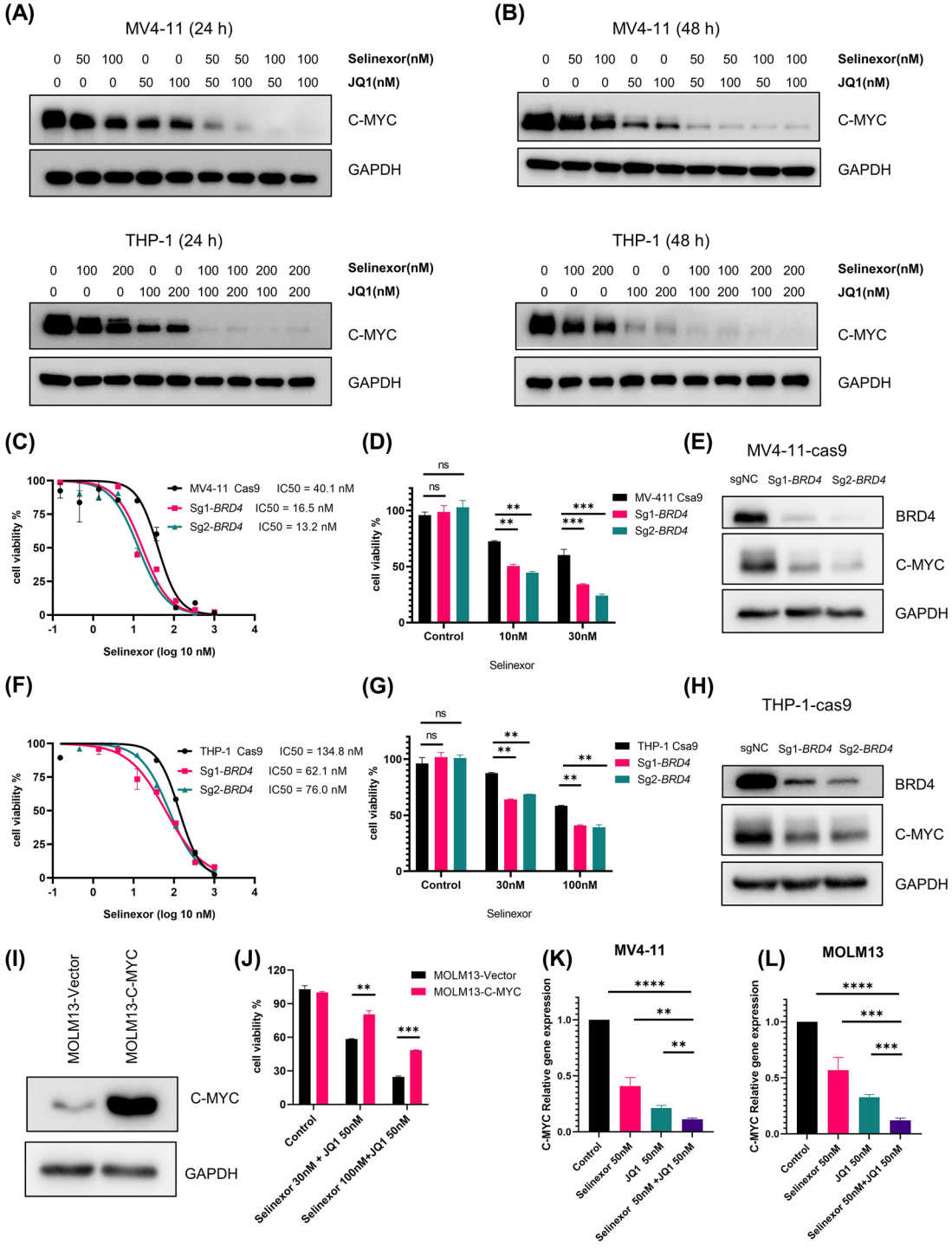

Fig. 3 Selinexor and JQ1 regulated the expression of C-MYC. (**A**-**B**) Expression levels of C-MYC at different concentrations of Selinexor and JQ1 in AML cells, respectively in cells MV4-11 and THP-1 at 24 h (**A**) and 48 h (**B**). (**C**) Detect the IC50 concentration of Selinexor in MV4-11 cells with scramble or *BRD4*-SgRNA. (**D**) Cell viability of MV4-11 cells with scramble or *BRD4*-SgRNA treated with different doses of Selinexor. (**E**) Expression levels of BRD4 and C-MYC proteins in MV4-11 cells with scramble or *BRD4*-SgRNA. (**F**) Detect the IC50 concentration of Selinexor in cells THP-1 cells with scramble or *BRD4*-SgRNA. (**G**) Cell viability of THP-1 cells with scramble or *BRD4*-SgRNA treated with different doses of Selinexor. (**H**) Expression levels of BRD4 and C-MYC proteins in THP-1 cells with scramble or *BRD4*-SgRNA. (**I**) Protein expression levels of C-MYC in MOLM13 cells transfected with vector or overexpressed C-MYC plasmid. (**J**) Cell viability of MOLM13 cells with scramble or C-MYC treated with different doses of Selinexor and JQ1. (**K**-**L**) RNA expression of C-MYC in MV4-11 (**K**) and MOLM13 (**L**) cells treated with different doses of Selinexor(50nM) and JQ1(50nM). All experiments were performed with at least three independent replicates

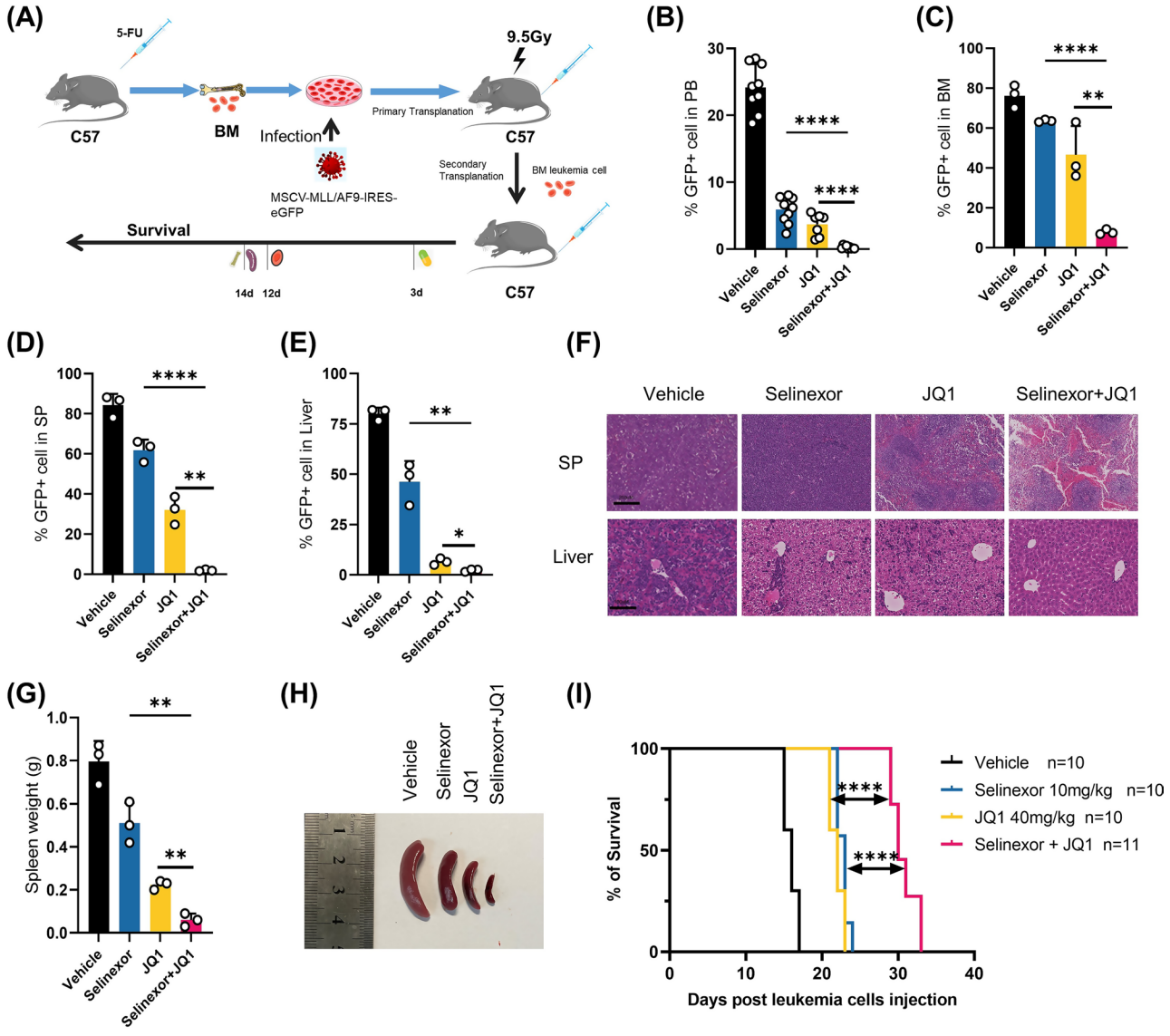

Fig. 4 The efficacy of Selinexor and JQ1 in a mouse model of bone marrow transplantation. (**A**) Diagram of the MLL-AF9 mouse model. (**B**-**E**) The proportion of GFP-positive cells in different tissues after treatment with Selinexor (10 mg/kg) and JQ1 (40 mg/kg), respectively in PB (**B**), BM (**C**), SP (**D**) and Liver (**E**). (**F**) Pathological morphological pictures of the spleen and liver treatment with Selinexor and JQ1. (**G**-**H**) Spleen weight (**G**) and morphological size (**H**) after treatment with Selinexor and JQ1. (**I**) Survival curves of mice after treatment with Selinexor and JQ1. *, $p < 0.05$; **, $p < 0.01$; ***, $p < 0.001$

of mice in the combination drug group could be further extended (Fig. 4I).

To further test the efficacy of JQ1-Selinexor combination therapy, we constructed a MOLM13 cell line-derived xenograft (CDX) model (Fig. 5A). The number of hCD45-positive tumor cells in the PB, BM and spleen were significantly reduced in the combination drug group (Fig. 5B-D and S7). The weight and size of the spleens were significantly reduced in the combination drug group (Fig. 5E-F). The spleen structure also gradually returned to normal after treatment (Fig. 5G). The mice treated with combination drugs had longer survival time (Fig. 5H). Further, the c-myc protein expressions in BM cells of mice were reduced after treatment (Fig. 5I). To assess drug toxicity, we administered JQ1 daily for 10 days and selinexor every other day to healthy BALB/c mice, with complete blood counts monitored every 3 days. The results revealed that the combination therapy showed moderate effects on neutrophil counts but minimal impact on platelet levels (Figure S8).

The efficacy of JQ1 and Selinexor in patient models

To further verify whether JQ1 and Selinexor are still effective in patients, we tested them in mononuclear tumor cells from the bone marrow of AML patients. We collected bone marrow mononuclear cells from 7 AML patients and sequenced the IC50 concentrations of different drugs (Figure S9). The experimental results showed

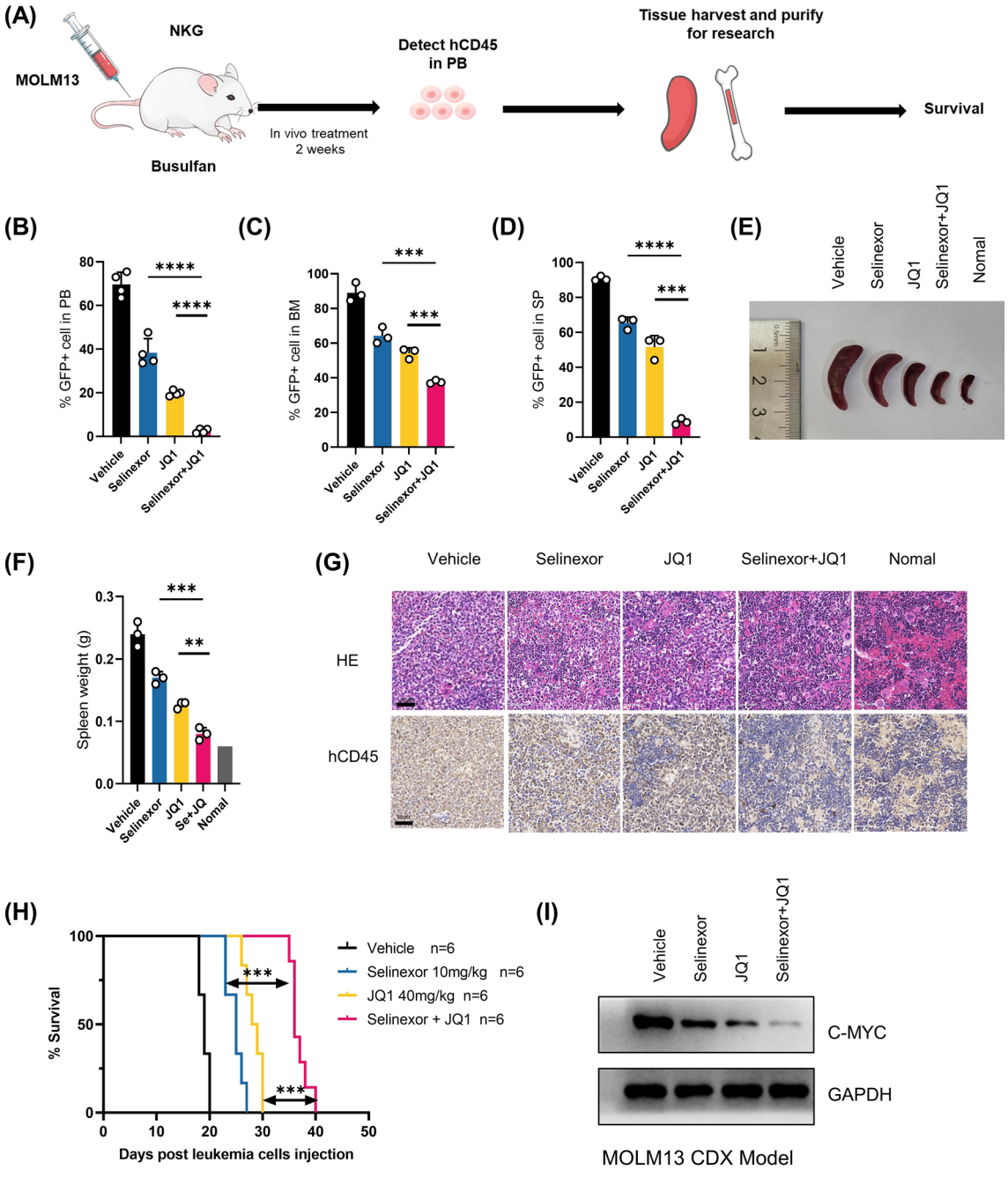

Fig. 5 The efficacy of Selinexor and JQ1 in MOLM13 cell line-derived xenograft (CDX) model. (**A**) Diagram of the MOLM13 CDX model. (**B**-**D**) The proportion of GFP-positive cells in different tissues after treatment with Selinexor (10 mg/kg) and JQ1 (40 mg/kg) in PB (**B**), BM (**C**) and SP (**D**). (**E**-**F**) Spleen morphological size (**E**) and weight (**F**) after treatment with Selinexor and JQ1. (**G**) Pathological morphological pictures of the spleen and liver treated with Selinexor and JQ1. (**H**) Survival curves of mice after treatment with Selinexor and JQ1. (**I**) Protein expression levels of C-MYC in BM cells of MOLM13 CDX model after treatment with Selinexor and JQ1. *, $p < 0.05$; **, $p < 0.01$; ***, $p < 0.001$

that primary AML cells had varying degrees of response to different concentrations of JQ1 and Selinexor (Fig. 6A, E and I and S10). In addition, the inhibition rate heatmap showed that there was a significant dose-dependency for JQ1 and Selinexor; as the drug concentration increased, the killing ability against AML tumor cells became stronger (Fig. 6B, F and J and S10). The synergy simulation curve indicated that JQ1 and Selinexor exhibited varying degrees of synergistic effects at any effective concentration with the synergy index lower than 1 (Fig. 6C, G and K and S10). Moreover, the HSA synergy simulation scores also yielded consistent results (Fig. 6D, H and L and S10). Mechanistically, we found that after drug treatment, the level of C-MYC protein in AML tumor cells decreased,

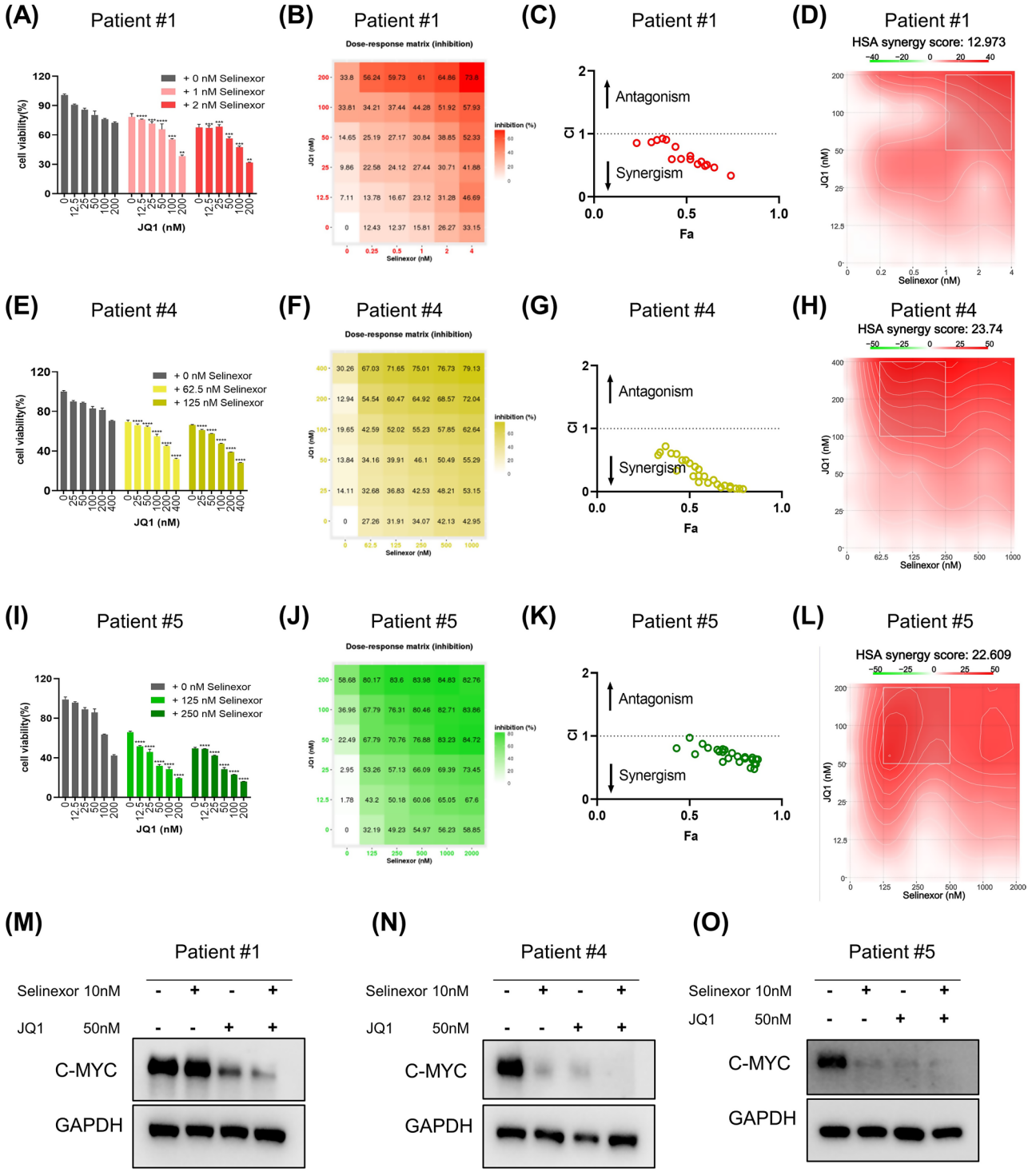

Fig. 6 The efficacy of Selinexor and JQ1 in primary patient cells. Cell viability assays under the influence of different concentrations of Selinexor and JQ1, respectively in patient 1# (**A**), patient 4# (**E**) and patient 5# (**I**). Inhibition rate heat map at different concentrations of Selinexor and JQ1, respectively in cells patient 1# (**B**), patient 4# (**F**) and patient 5# (**J**). Drug synergy index at different concentrations of Selinexor and JQ1 in different AML cells, respectively in cells patient 1# (**C**), patient 4# (**G**) and patient 5# (**K**). The HSA scores for these two drugs in patient 1# (**D**), patient 4# (**H**) and patient 5# (L). (**M**-**O**) Expression levels of C-MYC at different concentrations of Selinexor and JQ1 in patient 1# (**M**), patient 4# (**N**) and patient 5# (**O**) at 24 h. All experiments were performed with at least three independent replicates

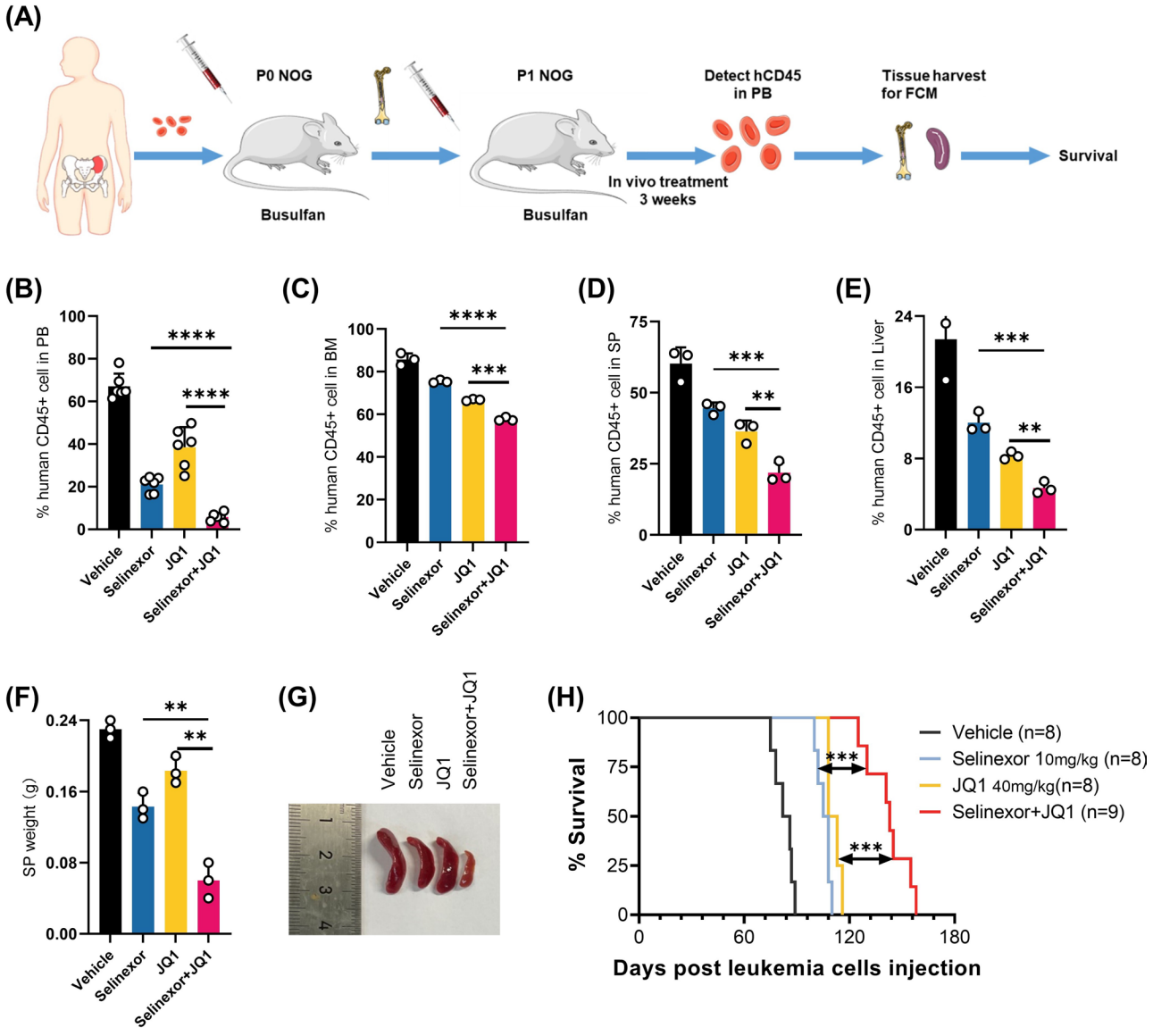

Fig. 7 The efficacy of Selinexor and JQ1 in a PDX mouse model. (**A**) Diagram of the PDX mouse model. the P1 NOG mice were randomly divided into four groups: vehicle, Selinexor (10 mg/kg), JQ1 (40 mg/kg) or Selinexor with JQ1. (**B**-**E**) The proportion of GFP-positive cells in different tissues after treatment with Selinexor and JQ1, respectively in PB (**B**), BM (**C**), SP (**D**) and Liver (**E**). (**F**-**G**) Spleen weight (**F**) and morphological size (**G**) after treatment with Selinexor and JQ1. (H) Survival curves of mice after treatment with Selinexor and JQ1. *, $p < 0.05$; **, $p < 0.01$; ***, $p < 0.001$

and it decreased even more after the combination of the two drugs (Fig. 6M-5O).

Subsequently, to further verify our hypothesis, we injected primary AML cells into NOG mice, ultimately establishing a humanized mouse PDX model (Fig. 7A). By using humanized CD45 (hCD45) to lable AML tumor cells, we compared the levels of hCD45 in hematopoietic tissues and the survival time of mice after medication at appropriate times. Consistent with the results from cell lines and bone marrow transplantation model mice, a single drug could reduce the proportion of hCD45-positive AML tumor cells in peripheral blood, bone marrow, spleen, and liver to a certain extent (Fig. 7B-E). The proportion of hCD45 tumor cells infiltrating in these tissues decreased more significantly after the combination of the two drugs (Fig. 7B-E). This suggests that the combination of JQ1 and Selinexor may have an advantage in leukemia invasion. The spleen weight and size of the PDX mice were also smaller after combined medication (Fig. 7F-G). And the survival time of mice in the combination drug group was significantly prolonged (Fig. 7H).

Discussion

The present study provides compelling evidence for the synergistic antileukemic effects of JQ1 and Selinexor in both in vitro and in vivo models of acute myeloid

leukemia (AML). These findings not only shed light on the potential of combination therapies in improve patient outcomes but also offer new insights into the molecular mechanisms underlying AML pathogenesis and treatment.

The synergistic cytotoxicity observed when JQ1 and Selinexor are used in combination is striking. This effect was consistent across multiple AML cell lines. For example, in the SAILOR trial which assessed Selinexor in relapsed/refractory AML patients, the complete remission (CR) rate was only about 10% [12]. In contrast, our study showed that in Kasumi-1 cells, the combination of JQ1 and Selinexor at specific concentrations could achieve an inhibitory rate over 85%, indicating a more powerful cytotoxic effect. The ability of JQ1 and Selinexor to jointly inhibit the expression of C-MYC is a key mechanism underlying their synergistic effects. MYC is a well-known oncogene that plays a crucial role in cell proliferation, differentiation, and apoptosis [21]. By concurrently targeting the expression of C-MYC, JQ1 and Selinexor may disrupt the oncogenic signaling pathways that drive AML progression. This finding is supported by the observed decrease in MYC protein expression levels following the combined use of both drugs [20, 22, 23]. For instance, in a study of AML patients treated with a different drug regimen aimed at targeting oncogenes, only a minor decrease in MYC expression was detected, while our combination therapy led to a more substantial reduction [12, 22].

The in vivo studies conducted using an MLL-AF9 bone marrow transplantation model provide further validation of the efficacy of JQ1 and Selinexor. The significant reduction in tumor cell burden observed in these mice, especially in the combined drug group, underscores the potential of this drug combination as a viable therapeutic option for AML patients. The ability of JQ1 and Selinexor to eradicate tumor cells outside the bone marrow, as evidenced by the reduced number of GFP^+ tumor cells in the spleen and liver, is particularly noteworthy. This finding suggests that this drug combination may be effective in targeting extramedullary disease, which is often associated with poor prognosis in AML patients [24]. In a clinical case series of AML patients with extramedullary infiltration who received standard chemotherapy, only 30% had a significant reduction in extramedullary tumor burden [25], while in our mouse model, the combination drug treatment showed a much better outcome.

The efficacy of JQ1 and Selinexor was also demonstrated in patient models. In our study involving 7 newly diagnosed AML patients in which we tested different concentrations of these drugs, primary AML cells exhibited varying degrees of response. The significant dose-dependency observed for both drugs further highlights the potential of optimizing their dosing regimens to achieve maximal therapeutic efficacy. Similar dose-response relationships have been observed in other clinical studies on different AML drugs. For example, in the quizartinib trials for AML patients with FLT3 mutations, different doses led to different response rates, and optimizing the dose improved the therapeutic outcome [26, 27]. The humanized mouse PDX model used in this study provided additional validation of the in vitro findings, demonstrating the ability of JQ1 and Selinexor to reduce the proportion of hCD45 positive AML tumor cells in various hematopoietic tissues.

Both cell line studies and clinical trial data indicate that XPO1 inhibitors exhibit limited efficacy as monotherapy in p53-mutated cases [11]. The application of JQ1-Selinexor combination therapy in AML represents our first reported study. We have provided detailed genetic mutation profiles of AML patients (Table S1), and current data suggest that this combination exerts synergistic effects across different genetic backgrounds. One limitation is the relatively small sample size in the patient-related experiments. Only 7 AML patients were involved in the test of drugs on mononuclear tumor cells from bone marrow. This small sample size may not be fully representative of the entire AML patient population. Our study's smaller sample size might have overlooked some of these variations. This indicates that a larger sample is necessary to better understand the variability in patient responses and confirm the generalizability of our results.

Conclusion

The present study provides strong evidence for the synergistic antileukemic effects of JQ1 and Selinexor in AML. These findings have important implications for the development of novel combination therapies that can improve patient outcomes. Future studies should focus on optimizing the dosing regimens and exploring the potential of this drug combination in other hematologic malignancies.

Supplementary Information

The online version contains supplementary material available at https://doi.org/10.1186/s12967-025-06525-z.

Supplementary Material 1

Acknowledgements

We especially thank Si-Yuan He (The University of Texas MD Anderson Cancer Center) for helping perform analysis of samples.

Authors' contributions

Pei-Hong Wang and Chu-Hong Hu performed basic and murine experiment; Jia-Qi Fan and Jia-Jun He performed bioinformatics analyses; Ting-Fen Deng interpreted data; Yan-Li Xu and Si-Yuan He performed guidance on flow cytometry experiments and flow cytometry data analysis.; Yu-Jun Dai and Pei-Hong Wang edited the paper; Shun-Qing Wang conceived and oversaw the study, interpreted data, and wrote the paper.-cell sequen

Funding
This work was supported by National Natural Science Foundation of China (82000144 and 82400204), Guangzhou Basic and Applied Basic Research Foundation (202201011458), Guangzhou Health Technology Project (20231A011012), Guangzhou Municipal Science and Technology Project (2024A03J1022 and 2023A04J0616) and GuangDong Basic and Applied Basic Research Foundation (2023A15115110992).

Data availability
All the data obtained and/or analyzed in the current study were available from the corresponding authors on reasonable request.

Declarations

Ethics approval and consent to participate
This work has been approved by Ethnics Committee of Guangzhou First People's Hospital.

Consent for publication
All authors give consent for the publication of manuscript.

Competing interests
The authors declare no competing financial interests.

Received: 7 February 2025 / Accepted: 21 April 2025
Published online: 08 May 2025

References

1. Molica M, et al. Maintenance therapy in AML: the past, the present and the future. Am J Hematol. 2019;94(11):1254–65.
2. Mohamed Jiffry MZ, et al. A review of treatment options employed in relapsed/refractory AML. Hematology. 2023;28(1):2196482.
3. Forsberg M, Konopleva M. AML treatment: conventional chemotherapy and emerging novel agents. Trends Pharmacol Sci. 2024;45(5):430–48.
4. Azizian NG, Li Y. XPO1-dependent nuclear export as a target for cancer therapy. J Hematol Oncol. 2020;13(1):61.
5. Deng M, et al. XPO1 expression worsens the prognosis of unfavorable DLBCL that can be effectively targeted by Selinexor in the absence of mutant p53. J Hematol Oncol. 2020;13(1):148.
6. Binder AF, et al. Impacting T-cell fitness in multiple myeloma: potential roles for Selinexor and XPO1 inhibitors. Front Immunol. 2023;14:1275329.
7. Long H et al. Azacitidine is synergistically lethal with XPO1 inhibitor Selinexor in acute myeloid leukemia by targeting XPO1/eIF4E/c-MYC signaling. Int J Mol Sci. 2023;24(7).
8. Wang Y, et al. CDK4/6 Inhibition augments anti-tumor efficacy of XPO1 inhibitor Selinexor in natural killer/T-cell lymphoma. Cancer Lett. 2024;597:217080.
9. Landes JR, et al. The efficacy of Selinexor (KPT-330), an XPO1 inhibitor, on non-hematologic cancers: a comprehensive review. J Cancer Res Clin Oncol. 2023;149(5):2139–55.
10. Martino EA, et al. Selinexor in multiple myeloma. Expert Opin Pharmacother. 2024;25(4):421–34.
11. Garzon R, et al. A phase 1 clinical trial of single-agent Selinexor in acute myeloid leukemia. Blood. 2017;129(24):3165–74.
12. Klement P, et al. Molecular response patterns in relapsed/refractory AML patients treated with Selinexor and chemotherapy. Ann Hematol. 2023;102(2):323–8.
13. Bhatnagar B, et al. Phase 1 study of Selinexor in combination with salvage chemotherapy in adults with relapsed or refractory acute myeloid leukemia. Leuk Lymphoma. 2023;64(13):2091–100.
14. Sweet K, et al. A 2:1 randomized, open-label, phase II study of Selinexor vs. physician's choice in older patients with relapsed or refractory acute myeloid leukemia. Leuk Lymphoma. 2021;62(13):3192–203.
15. Sweet K, et al. Phase I clinical trial of Selinexor in combination with Daunorubicin and cytarabine in previously untreated Poor-Risk acute myeloid leukemia. Clin Cancer Res. 2020;26(1):54–60.
16. Wang AY, et al. A phase I study of Selinexor in combination with high-dose cytarabine and Mitoxantrone for remission induction in patients with acute myeloid leukemia. J Hematol Oncol. 2018;11(1):4.
17. Zhang W, et al. Combinatorial targeting of XPO1 and FLT3 exerts synergistic anti-leukemia effects through induction of differentiation and apoptosis in FLT3-mutated acute myeloid leukemias: from concept to clinical trial. Haematologica. 2018;103(10):1642–53.
18. Guo HZ, et al. Leukemic progenitor cells enable immunosuppression and post-chemotherapy relapse via IL-36-inflammatory monocyte axis. Sci Adv. 2021;7(41):eabg4167.
19. Sanjana NE, Shalem O, Zhang F. Improved vectors and genome-wide libraries for CRISPR screening. Nat Methods. 2014;11(8):783–4.
20. Bauer K, et al. BRD4 degraders May effectively counteract therapeutic resistance of leukemic stem cells in AML and ALL. Am J Hematol. 2024;99(9):1721–31.
21. Tang R, et al. c-MYC amplification in AML. J Assoc Genet Technol. 2021;47(4):202–12.
22. Call SG, et al. Targeting oncogenic super enhancers in MYC-Dependent AML using a small molecule activator of NR4A nuclear receptors. Sci Rep. 2020;10(1):2851.
23. Yu H, et al. Venetoclax enhances DNA damage induced by XPO1 inhibitors: A novel mechanism underlying the synergistic antileukaemic effect in acute myeloid leukaemia. J Cell Mol Med. 2022;26(9):2646–57.
24. Strickland SA, Vey N. Diagnosis and treatment of therapy-related acute myeloid leukemia. Crit Rev Oncol Hematol. 2022;171:103607.
25. Yang LX, et al. C1Q labels a highly aggressive macrophage-like leukemia population indicating extramedullary infiltration and relapse. Blood. 2023;141(7):766–86.
26. Erba HP, et al. Quizartinib plus chemotherapy in newly diagnosed patients with FLT3-internal-tandem-duplication-positive acute myeloid leukaemia (QuANTUM-First): a randomised, double-blind, placebo-controlled, phase 3 trial. Lancet. 2023;401(10388):1571–83.
27. Joshi SK, et al. The FLT3(N701K) mutation causes clinical AML resistance to gilteritinib and triggers TKI sensitivity switch to Quizartinib. Am J Hematol. 2023;98(12):E364–8.

Publisher's note